

# Methods for experimental design, central composite design and the Box–Behnken design, to optimise operational parameters: A review

N. Szpisják-Gulyás<sup>1</sup>, Aws N. Al-Tayawi<sup>1</sup>, Zs. H. Horváth<sup>2</sup>, Zs. László<sup>3</sup>,  
Sz. Kertész<sup>3\*</sup>  and C. Hodúr<sup>3</sup>

<sup>1</sup> Doctoral School of Environmental Sciences, University of Szeged, Szeged, Hungary

<sup>2</sup> Department of Mechanical Engineering, Faculty of Engineering, University of Szeged, Szeged, Hungary

<sup>3</sup> Department of Biosystems Engineering, Faculty of Engineering, University of Szeged, Szeged, Hungary

## REVIEW PAPER

Received: September 13, 2023 • Accepted: November 9, 2023

Published online: November 29, 2023

© 2023 The Author(s)



## ABSTRACT

In recent years response surface analysis has been increasingly used to optimise membrane separation. It has many advantages, such as reducing the number of experiments to be performed, which requires lower energy consumption and significantly less laboratory work. For more accurate data analysis and forecasting, mathematical models are used that analyse the relevance of the factors examined and the interaction effects between the factors. In this research, two experimental designs that use response surface methodology are presented, namely, the central composite design and the Box–Behnken design. After the general characterisation of the experimental designs, their application in membrane technology is presented.

## KEYWORDS

Box–Behnken design, central composite design, membrane technology, optimisation, response surface methodology

\* Corresponding author. Tel.: +36 62 546 580. E-mail: kertesz@mk.u-szeged.hu

## 1. INTRODUCTION

Response surface methodology (RSM) is a mathematical and statistical method widely used to model and analyse various processes where the desired response is influenced by various variables and the goal is to optimise the response. They are very effective because they take into account main effects and interaction effects with a minimum number of experiments, thus clarifying the causal relationship between factors and responses. Experiment design and optimisation methodology play an important role in modern research and development. The traditional approach to the optimisation problem is the one-factor method, where we examine the effect of one variable while keeping the other variables at a constant level (Bezerra et al., 2008). In order to achieve optimal conditions, this procedure is repeated with other variables. The main disadvantage of this method is that it does not represent the interactive effects between the investigated variables, so it cannot provide the full effect of the variables on the process. In addition, the one-factor approach increases the number of experiments required to conduct the research, so it would be costly and time-consuming (Ba and Boyaci, 2007; Bezerra et al., 2008). Consequently, factor optimisation procedures using multivariate techniques have been encouraged, as they are faster, more economical, and more efficient and allow the simultaneous optimisation of more than one variable (Ferreira et al., 2007; Leardi, 2009; Tarley et al., 2009; Kemény et al., 2017). Response surface methodologies are multivariate techniques that mathematically fit the experimental range under consideration in theoretical design via a response function (Myers and Montgomery, 1995). It was originally developed by Box and Wilson (1951) to improve yields in the chemical and other processing industries. RSM is now used to optimise systems in many fields due to its high efficiency, such as electronics, biotechnology, aerospace, automotive, life sciences, agricultural environment, and manufacturing (Anderson-Cook et al., 2009; Zolgharnein et al., 2013).

In RSM, mathematical models generated using experimental design data determine the relationships between independent variables (factors) and dependent variables (responses). These models are used to analyse the effects and interactions of independent variables on responses and to optimise the process. The application of RSM as an optimisation tool consists of several steps. These include (i) selecting independent variables and their ranges, (ii) selecting the experimental design and conducting the experiments, (iii) creating a linear regression model equation based on the experimental results, (iv) checking the appropriateness of the model, and (v) graphing the model representation and achieving optimal conditions (Nair et al., 2014).

Response surface designs can use first-order (linear) or second-order (quadratic) or higher-order (cubic and quartic) model fitting. Higher-order models are always the most suitable for analysing possible interactions between factors, but linear, quadratic, and cubic interactions are also possible. The typical model equation (Eq. (1)) for response surface designs is presented, which explains different model terms corresponding to the degree of interactions between the factor levels.

$$Y = \beta_0 + \beta_1 X_1 + \beta_2 X_2 + \beta_3 X_1^2 + \beta_4 X_2^2 + \beta_5 X_1 X_2 \quad (1)$$

where  $\beta_0$  the constant term,  $\beta_1 - \beta_2$  the coefficients of the linear model terms,  $\beta_3 - \beta_4$  the coefficient of quadratic model terms,  $X_1 - X_2$  the model terms.

The two most common designs used in response surface modeling are the central composite design and the Box–Behnken design. Membrane technology is a field where experimental design is widely used for optimisation, so this paper aims to introduce the theory and applications of Box–Behnken design and central composite design in the fields of membrane technology.



## 2. BOX-BEHNKEN DESIGN

The Box–Behnken design (BBD) is a widely used response surface methodology design that is particularly useful for establishing cause-and-effect relationships between factors and responses in experiments. It was developed by George E. P. Box and Donald Behnken in 1960 ([Box and Behnken, 1960](#)).

Box–Behnken designs are a class of rotatable or nearly rotatable second-order designs based on three-level incomplete factorial designs. For three factors, the graphical representation is a cube consisting of a center and the middle points of the edges, the points being located on the surface of a sphere, as shown in [Fig. 1](#). The coded values for three factors are shown in [Table 1](#). To form the response surface, BBD requires three levels (−1, 0, and +1) and can be used for factors between 3 and 21. The center points are marked with “0” and are used to generate quadratic model terms and to analyse the second-order interaction effect between the factors.

The number of experiments ( $N$ ) required for the development of BBD is defined as follows (Eq. (2)):

$$N = 2k * (k-1) + C_0 \quad (2)$$

where  $k$  is a number of factors and  $C_0$  is the number of central points.

One of the advantages of BBD is that it does not contain combinations in which all factors are at the highest or lowest levels at the same time, so in this case it is not necessary to perform measurements in extreme situations (the vertices of the cube).

The Box–Behnken design is widely used in membrane technology. Some of the experiments are related to membrane fouling, which is the main drawback of membrane technology and which causes a decrease in system performance, mainly observed in lower permeate flux or changed membrane selectivity. The degree of fouling is highly dependent on the membrane properties, the feed solution, and the hydrodynamics of the process. [Alventosa-DeLara et al. \(2014\)](#), [Kyllönen et al. \(2005\)](#), and [Peeva et al. \(2012\)](#) investigated the problem of membrane fouling during ultrafiltration of dye-containing wastewater. They investigated the cleaning efficiency that can be achieved by changing the transmembrane pressure (TMP)

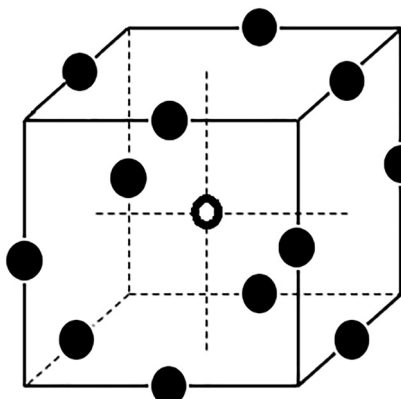


*Fig. 1.* Box–Behnken design for three factors



Table 1. Box–Behnken design of three factors

Experiment	x <sub>1</sub>	x <sub>2</sub>	x <sub>3</sub>
1	−1	−1	0
2	+1	−1	0
3	−1	+1	0
4	+1	+1	0
5	−1	0	−1
6	+1	0	−1
7	−1	0	+1
8	+1	0	+1
9	0	−1	−1
10	0	+1	−1
11	0	−1	+1
12	0	+1	+1
13 (C)	0	0	0
14 (C)	0	0	0
15 (C)	0	0	0
16 (C)	0	0	0

(0.5, 1.5, and 2.5 bar), the crossflow velocity (1, 2, and 3 m s<sup>−1</sup>) and the ultrasound power level (40%, 70%, and 100%). The crossflow velocity appeared to be the most influencing factor, followed by the TMP and the ultrasound power level. The maximum estimated cleaning efficiency was 32.19%, which can be achieved with 1.1 bar TMP, 3 m s<sup>−1</sup>, and 100% ultrasound power.

During ultrafiltration (UF) of pomegranate juice, Baklouti et al. (2013) investigated the flux behavior with a resistance-in-series model, which included the resistance of the membrane, fouling, and solute concentration polarisation. A Box–Behnken experimental design with three parameters, namely transmembrane pressure, feed rate, and temperature, was used to determine the relationships between operating parameters and the efficiency of ultrafiltration and to determine the optimal conditions. The three response functions are the fouling resistance (R<sub>f</sub>), the resistance due to concentration polarisation (R<sub>cp</sub>), and the permeate flux. The optimal conditions were: 3 bar TMP, 0.95 L min<sup>−1</sup> feed rate, and 30 °C temperature. Then the R<sub>f</sub> was 18%, the R<sub>cp</sub> is 72%, and the optimal value of the permeate flux was 19 L h<sup>−1</sup> m<sup>−2</sup>.

Figueroa et al. (2011) analysed the performance of polysulfone ultrafiltration hollow fiber membranes in the clarification of orange press liquor. Transmembrane pressure (0.2–1.4 bar), temperature (15–35 °C), and feed flow-rate (85–245 L h<sup>−1</sup>) were varied between the given ranges. They investigated how these factors affect permeate flux, fouling index, and blocking index. The quadratic values of TMP, temperature, and feed flow rate showed significant effects on the UF membrane performance. The goal was to maximise permeate flux and minimise fouling index values. For an overall desirability of 0.76, permeate fluxes were estimated to be 23.7 kg m<sup>−2</sup> h<sup>−1</sup> and the fouling index as 48.0% under optimised operating variables (TMP = 1.4 bar, temperature = 15 °C, and feed flow-rate = 167.7 L h<sup>−1</sup>).

In another group of experiments, the Box–Behnken experimental design was used in membrane technology separation procedures, because their operation is simple, there is no phase change and no need to add any chemicals to achieve the expected separation.



These properties have made them suitable as substitutes for other separation and treatment technologies while meeting their separation objectives (Madaeni and Samieirad, 2010; Miao et al., 2013). Ultrafiltration was used as a separation process to purify and concentrate solutions according to Xue et al. (2019). A Box–Behnken design was used to investigate the effect of ultrafiltration pH, temperature, and pressure on the extraction rate for Chinese yam polysaccharide (CYP). The optimal parameters were a temperature of 20 °C, a pH of 6.5, and a pressure of 0.03 MPa, at which time the experimental extraction ratio of CYP was 88.7%. Malaisamy et al. (2000) also used the BBD experimental design for evaluation of separation operations. Membranes containing different concentrations of polyethylene glycol were prepared to investigate vitamin B2 separation. The investigated parameters were additive concentration, feed concentration, and solvent evaporation time. The maximum vitamin B2 retention was 56.25%. The effect of process variables on the performance of Micellar Enhanced Ultrafiltration (MEUF) for the removal of nickel ions from aqueous solutions was studied by Lin et al. (2020). The process variables were pressure, nickel concentration, sodium dodecyl sulfate (SDS) concentration, and molecular weight cut-off (MWCO), and quadratic models for nickel rejection rate and flux were generated using RSM. Optimum conditions for maximum nickel removal and flux to remove 1 mM nickel ion were: pressure = 30 psi, SDS = 10.05 mM, and MWCO = 10 kDa, giving a retention rate of 98.16% and 119.20 L h<sup>-1</sup> m<sup>-2</sup> results in a flux.

Salehi et al. (2019) analysed the MEUF process for the removal of the drug sotalol hydrochloride from synthetic wastewater using RSM, and also investigated the effects of surfactant concentration, TMP, and pH on rejection and permeate flux. The results of the experiments showed that the retention of the sotalol hydrochloride active ingredient using an ultrafiltration membrane was a maximum of 32.41%, while this amount increased to 96.82% with the addition of the surfactant and the formation of micelles.

Aloulou et al. (2022) optimised the filtration of oily wastewater, while Sivakumar et al. (1999) used cellulose-acetate-polyurethane blend membranes for effective aqueous separation by ultrafiltration. An experimental design was used to develop an additive mathematical relationship between time and pressure. The new mixture membrane showed better results in the separation of protein (BSA) (96%).

In the food industry, the Box–Behnken experimental design was mainly used to optimise extraction and drying processes. The two most commonly used variables in extraction processes are temperature and time. Fan et al. (2008) investigated the extraction of anthocyanins from purple sweet potatoes (*Ipomoea batatas* (L.) Lam). In addition to temperature and time, the third parameter that was changed was the solid-liquid ratio. As a response function, the yield anthocyanin and colour coordinates were investigated. In another study, Prakash Maran and Manikandan (2012) investigated the aqueous extraction of pigments from the prickly pear (*Opuntia ficus-indica*) fruit. In this case, the third parameter was the weight of the fruit and the yield of betacyanin and betaxanthin was optimised. The extraction of acid-soluble collagen from grass carp (*Ctenopharyngodon idella*) was optimised by L. Wang et al. (2008), the third parameter was the concentration of acetic acid. Xie et al. (2012) conducted a study to examine the impact of ultrasound-assisted extraction on the antimicrobial and antioxidant properties of polysaccharides derived from *Cyclocarya paliurus* (Batal.) Iljinskaja.

Some applications of the Box–Behnken design in membrane technology and the food industry are summarised in Table 2.



Table 2. Summary of some application of Box-Behnken design in the membrane technology and food industry

Application	Independent variables	Response(s) studied	Reference
The ultrasound-enhanced cleaning of an ultrafiltration ceramic membrane.	Transmembrane pressure, cross-flow velocity, ultrasound power level	Cleaning efficiency	Alventosa et al. (2014)
Optimising operating conditions in ultrafiltration fouling of pomegranate juice.	Transmembrane pressure, feed flow rate, temperature	Fouling resistance, polarised layer resistance, membrane resistance, permeate limit flux	Baklouti et al. (2013)
Optimisation for permeate flux and fouling index.	Transmembrane pressure, temperature, feed flow rate	Permeate flux, fouling index, blocking index	Figueroa et al. (2011)
Optimisation of the ultrafiltration-assisted extraction of Chinese yam polysaccharide.	Ultrafiltration pH, ultrafiltration temperature, ultrafiltration pressure	Extraction rate	Xue et al. (2019)
Performance optimisation of polysulfone ultrafiltration membranes for riboflavin separation.	Additive concentration, feed concentration, evaporation time	Vitamin B <sub>2</sub> rate	Malaisamy et al. (2000)
Micellar-Enhanced Ultrafiltration to remove nickel ions.	Pressure, Ni concentration, Surfactant sodium dodecyl sulfate (SDS) concentration, molecular weight cut-off (MWCO)	Nickel rejection rates, permeate flux	Lin et al. (2020)
Assessment of micellar-enhanced ultrafiltration process performance for removal of pharmaceutical contaminant from wastewater.	Surfactant sodium dodecyl sulfate (SDS) concentration, pH, transmembrane pressure	Permeate flux, rejection	Salehi et al. (2019)
To determine the optimised ultrafiltration conditions for industrial wastewater treatment loaded with oil and heavy metals generated from an electroplating industry.	Initial oil concentration, temperature, transmembrane pressure	Chemical oxygen demand, permeate flux	Aloulou et al. (2022)
Cellulose acetate-polyurethane ultrafiltration membranes for BSA separation.	Polyvinylpyrrolidone (PVP) concentration, time, rejection rate	Separation of BSA	Sivakumar et al. (1999)

(continued)



**Table 2.** Continued

Application	Independent variables	Response(s) studied	Reference
Optimising conditions for anthocyanins extraction from purple sweet potato.	Extraction temperature, time, solid-liquid ratio,	Anthocyanins yield, colour attributes (L*, C*, H)	Fan et al. (2008)
Optimisation of process parameters for aqueous extraction of pigments from prickly pear ( <i>Opuntia ficus-indica</i> ) fruit.	Extraction temperature, extraction time, mass of the fruit	Total betacyanin and betaxanthin contents	Prakash Maran and Manikandan (2012)
Optimisation of conditions for extraction of acid-soluble collagen from grass carp ( <i>Ctenopharyngodon idella</i> ).	Acetic-acid concentration, time, temperature	Acid-soluble collagen yield	Wang et al. (2008)
A <i>Cyclocarya paliurus</i> (Batal.) Iljinskaja ultrasound-assisted extraction of polysaccharides, antimicrobial and antioxidant effects.	Ratio of liquid to solid, temperature, time	Polysaccharides yield	Xie et al. (2012)

### 3. CENTRAL COMPOSITE DESIGN

The central composite design (CCD) is one of the most commonly used response surface design, which was introduced by Box and Wilson in 1951 as an alternative to the full-level factorial design (Box and Wilson, 1951). It applies a second-order (quadratic) model to the response variable without using a three-level factorial experiment, therefore widely used for experimental response surface optimisation. CCD is an extended form of three-level factorial design with star points or axial points. This is used when factorial designs detect curvature in the data, so it is necessary to expand from the previous linear design to a quadratic response surface design (Singh and Beg, 2013). In this context, CCD extends the factorial design by adding center points and star points, which allows for the estimation of the curvature effect (Hanrahan et al., 2005).

The CCD consists of three parts: factorial points, axial/star points, and center points. The factorial points contain a possible combination of points at two different levels ( $-1$ ,  $+1$ ) and have an important role in the estimation of main effects, linear interaction effects, and quadratic effects. The center points are one of the important points of the design that are represented with level “0”, their total number is between 3 and 5. These are used to generate quadratic model terms and to analyse the quadratic interaction effect between the factors. The axial or star points are CCD features only and are represented by  $-\alpha$ / $+\alpha$ . A CCD always contains twice as many star points as the number of factors in a design (Otto, 1999). The appropriate symmetry of the design is ensured by the value of “ $\alpha$ ”, which indicates the degree of rotatability. In general, the number of factors in CCD can range between 2 and 50 and requires 5 levels for each of the selected factors, which are  $-\alpha$ ,  $+\alpha$ ,  $-1$ ,  $0$ , and  $+1$ . In the case of three factors, Table 3 presents the coded values of the experimental design.



Table 3. Rotatable central composite design of three factors

Experiment	x <sub>1</sub>	x <sub>2</sub>	x <sub>3</sub>
1	-1	-1	-1
2	+1	-1	-1
3	-1	+1	-1
4	+1	+1	-1
5	-1	-1	+1
6	+1	-1	+1
7	-1	+1	+1
8	+1	+1	+1
9	- $\alpha$	0	0
10	+ $\alpha$	0	0
11	0	- $\alpha$	0
12	0	+ $\alpha$	0
13	0	0	- $\alpha$
14	0	0	+ $\alpha$
15 (C)	0	0	0
16 (C)	0	0	0
17 (C)	0	0	0
18 (C)	0	0	0

The number of experiments can be determined using the following equation (Eq. (3)):

$$N = 2^k + 2k + C_0 \quad (3)$$

where  $k$  is the number of factors,  $2^k$  is the number of factorial points,  $2k$  is the number of axial/star points and  $C_0$  the number of center points.

### 3.1. Rotatability in CCD

Rotatability is the property that allows constant variance prediction at all points that are equidistant from the design center (Malekzadeh and Fatemi, 2015). If the variance of the predicted values of Y is a function of the distance of a point from the center of the design the plan can be rotatable. Therefore, the value of  $\alpha$  depends on the number of experiments performed in the factorial part, which is given by the following equation (Eq. (4)) (Box and Wilson, 1951):

$$\alpha = (\text{number of factorial points})^{1/4} \quad (4)$$

If the factorial space is generated from a full factorial, the equation can be simplified (Eq. (5)):

$$\alpha = [2^k]^{\frac{1}{4}} \quad (5)$$

Table 4 provides some specific values of  $\alpha$  as a function of the number of factors that maintain the rotatability of CCDs. The  $\alpha$  is the distance of each axial point (star point) from the center of the CCD. If  $\alpha$  is less than one, the axial points are in the cube, if the value of  $\alpha$  is equal to one they are on the faces of the cube, and if the value of  $\alpha$  is greater than one they are located outside the cube (Draper and Lin, 1990).



Table 4. Relationship between the number of factors and value of “ $\alpha$ ” (Beg, 2021)

Number of factors	Factorial portion	Scaled value for $\alpha$ relative to $\pm 1$
2	$2^2$	$2^{2/4} = 1.414$
3	$2^3$	$2^{3/4} = 1.682$
2	$2^4$	$2^{4/4} = 2.000$
5	$2^{5-1}$	$2^{4/4} = 2.000$
5	$2^5$	$2^{5/4} = 2.378$
6	$2^{6-1}$	$2^{5/4} = 2.378$
6	$2^6$	$2^{6/4} = 2.828$

### 3.2. Types of CCD

CCDs can be classified into two main types based on the levels and positions of the axial/star points:

- **Rotatable central composite design (RCCD):** In this type of CCD, the axial/star points are not aligned with the plane of the factorial points. Instead, they are located at a distance ( $\alpha$ ) from the center of the design and can extend beyond the faces of the factorial cube. The main advantage of this design is its rotatability, which means that the design exhibits constant variance prediction at all points that are equidistant from the center. This property is desirable for robust and reliable analysis of the experimental data (Fig. 2a).
- **Face-centered central composite design (FCCD):** In this type of CCD, the axial/star points are aligned with the plane of the factorial points. The axial points are located at a specific distance ( $\alpha$ ) from the center of the design and lie on the faces of the factorial cube. In this design, the axial points are at the center of each face of the factorial space; therefore the levels  $-1/+1$  for factorial points are the same as the axial/star points and both points are on the same plane (Nekkanti et al., 2009). One advantage of FCCD is that it allows for efficient estimation of main effects and interactions, providing useful information about the linear and interaction effects of the factors. The design points are strategically placed on the faces of the factorial cube and in the center, allowing for a balanced and efficient exploration of the factor space. However, a potential weakness of FCCD is the poor accuracy in estimating pure

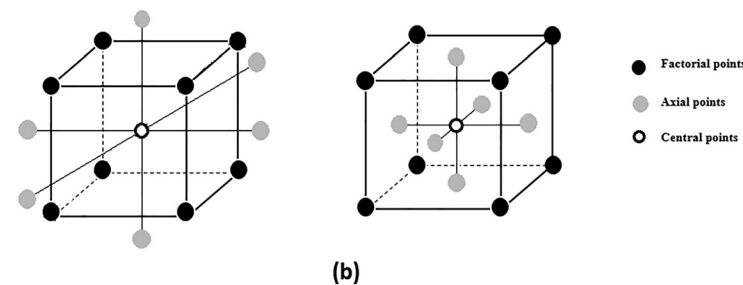


Fig. 2. (a): Rotatable central composite design (RCCD), (b): Face-centered central composite design (FCCD)



quadratic coefficients. Since the axial/star points are aligned with the plane of the factorial points, the design may not adequately capture the curvature effects. This limitation makes FCCD less suitable for accurately estimating pure quadratic terms in the response surface model (Fig. 2b).

CCD is widely used in the membrane separation optimisation process to determine the ideal state of the experimental parameters. CCD is a preferable method compared to other methods like Box–Behnken design etc., because the CCD methodology gives better information within or beyond the limits of the spinning process, while the BBD method does not give information about the spinning process limitations and cannot be built in two steps from the  $2^k$  design (Shakir et al., 2015).

Landaburu-Aguirre et al. (2010) used face centered central composite design to understand the concentration polarisation phenomenon and the effect of factors on heavy metal retention and permeate flux. Additionally, the recovery of the anionic surfactant sodium dodecyl sulfate was studied. The investigated factors were the following: pressure (P), nominal molecular weight limit (NMWL), heavy metal feed concentration ( $C_{Zn}$ ,  $C_{Cd}$ ), and SDS feed concentration ( $C_{SDS}$ ).

The rotatable central composite design was used in the works described below.

Krishnan et al. (2020) minimised the production cost of xylitol by optimising the xylose reductase (XR) enzyme purification process. Ultrafiltration was used for their experiments, as membrane-based processes play a critical role in the separation/purification of biotechnological products (Sharma and Bracewell, 2019). Operating conditions such as transmembrane pressure (TMP) and cross-flow velocity (CFV) affect the cleaning performance and the fouling phenomenon (Dereli et al., 2019). In addition to transmembrane pressure and cross-flow velocity, the third process variable was filtration time. Membrane permeability and xylitol content were investigated as response variables.

Sadeghian et al. (2015) investigated the ultrafiltration ability of the hollow fiber polyvinylidene fluoride membrane in an oil-in-water emulsion pretreated with polyaluminum chloride. A central composite design and a response surface method were used to optimise the operating variables: transmembrane pressure and velocity. The three response functions were permeate flux (PF), turbidity removal, and chemical oxygen demand (COD).

Candéa et al. (2015) studied the effect of process variables on the production of flaxseed oil emulsions by cross-flow membrane emulsification. The effects of transmembrane pressure, crossflow velocity, and surfactant concentration on dispersed phase flux, emulsion stability, and droplet size distribution and uniformity were evaluated.

C. Wang et al. (2016) used central composite design and the response surface method to predict and optimise a polyvinylidene fluoride (PVDF) membrane cleaning process. Four independent variables were taken into account (sodium hydroxide (NaOH) concentration, sodium hypochlorite (NaClO) concentration, citric acid concentration, and the duration of cleaning), and the cleaning efficiency was investigated as a response. Park et al. (2018) used CCD to predict the cleaning efficiency of a reverse osmosis (RO) membrane with organic-fouling, where the variables were the concentration of cleaning solution, the cleaning time, the flow rate, and the temperature.

MEUF was used by Vani et al. (2023) to remove fluoride using polyethersulfone (PES) based ultrafiltration membranes and a cationic surfactant (cetylpyridinium chloride-CPC) and by



Table 5. Summary of some application of Central composite design in the membrane technology and food industry

Application	Independent variables	Response (s) studied	Reference
Optimisation of cadmium and zinc removal from water samples by micellar-enhanced ultrafiltration.	Pressure, nominal molecular weight limit (NMWL), heavy metal feed concentration, sodium dodecyl sulfate (SDS) concentration	Permeate flux, heavy metal retention	Landaburu-Aguirre et al. (2010)
Optimisation of operating parameters for xylose reductase separation through ultrafiltration membrane.	Filtration time, transmembrane pressure, cross flow velocity	Membrane permeability, amount of xylitol	Krishnan et al. (2020)
The capability of ultrafiltration hollow fibre polyvinylidene fluoride membrane by polyaluminum chloride in pretreated oil-in-water emulsion.	Transmembrane pressure, velocity	Permeate flux, turbidity removal, chemical oxygen demand removal	Sadeghian et al. (2015)
The effect of process variables on the production of flaxseed oil emulsions by cross-flow membrane emulsification.	Transmembrane pressure, cross flow velocity, emulsifier concentration	Dispersed phase flux, droplet size, droplets' size uniformity (Span)	Candéa et al. (2015)
Prediction and optimisation of the chemical cleaning process of polyvinylidene fluoride (PVDF) ultrafiltration membranes.	Sodium hydroxide concentration, sodium hypochlorite concentration, citric acid concentration, cleaning duration	Cleaning efficiency	Wang et al. (2016)
Optimisation of chemical cleaning for reverse osmosis membranes.	Concentration of EDTA, cleaning time, temperature, flow rate	Flux recovery	Park et al. (2018)
Removal of fluoride by micellar enhanced ultrafiltration.	Surfactant concentration, pressure drop, time	Fluoride concentration	Vani et al. (2023)
Copper removal from aqueous solutions using micellar-enhanced ultrafiltration.	pH, surfactant concentration, surfactant/metal molar ratio	Copper rejection	Xiarchos et al. (2008)
Copper removal from aqua solutions using polymer assisted ultrafiltration.	Feed concentration of polyacrylic acid, ratio of polymer to copper, pH	Copper rejection	Cojocaru and Zakrzewska-Trznadel (2007)



**Table 5. Continued**

Application	Independent variables	Response (s) studied	Reference
Effect of various types of anions and anionic surfactants on the performance of micellar-enhanced ultrafiltration process in the removal of Pb(II) ions.	Lead concentration, NaCl concentration, lead salt, anionic surfactant	Lead removal	Abhari et al. (2022)
Optimisation of stabiliser usage conditions in oat milk production.	Stabiliser concentration, swelling time	Colour parameters ( $L^*$ , $a^*$ , $b^*$ , $\Delta E$ ), Rheological properties (yield stress, consistency index, fluid type)	Akal et al. (2023)
Optimisation of ultrasound-assisted extraction of natural pigment from annatto seeds.	Temperature, extraction time, duty cycle, seed to solvent ratio	Extraction yield, absorbance value	Yolmeh et al. (2014)
Extraction of natural dye from petals of Flame of forest ( <i>Butea monosperma</i> ) flower.	Time, temperature, mass of petals	Total amount of dye	Sinha et al. (2012)
Optimisation of the solvent extraction of bioactive compounds from <i>Parkia speciosa</i> pod.	Buffer to solid ratio, temperature, time	Total polyphenolic content, total flavonoid content, DPPH content, ABTS content, Ferric reducing/antioxidant power content	Gan and Latiff (2011)
Optimisation of extraction parameters of bioactive components from defatted marigold ( <i>Tagetes erecta</i> L.) residue.	Ethanol concentration, temperature, time	Total polyphenolic content, total flavonoid content, DPPH content, ABTS content	Gong et al. (2012)
Optimisation of microwave-assisted hot air drying conditions of okra.	Air velocity, air temperature, microwave power	Colour change, hardness, rehydration ratio, specific energy	Kumar et al. (2014)
Optimisation of process parameters for microwave vacuum drying of apple slices.	Microwave power, vacuum level, initial moisture content	Drying time, sensor quality, porosity	Han et al. (2010)



Xiarchos et al. (2008) to optimise the extraction of copper from aqueous solutions. Cojocaru and Zakrzewska-Trznadel (2007) also deals with the removal of copper ions from aqueous solutions. The work presents the application of RSM for the optimisation of dead-end and cross-flow polymer-assisted ultrafiltration (PAUF) using a polyacrylic acid (PAA) chelating agent. MEUF was used by Abhari et al. (2022) to remove  $Pb^{2+}$  ions from aqueous solution. The process was used to simultaneously maximise the retention of  $Pb^{2+}$  and the flux of permeates. SDS and sodium lauroyl sarcosine (Sarkosyl) were used as anionic surfactants.

In the food industry, the rotating center experimental design was used for optimise stabiliser and swelling time of oat in the production of oat milk (Akal et al., 2023). It was used for colour extraction by Yolmeh et al. (2014), who extracted pigments from annatto seeds using ultrasound, and Sinha et al. (2012), who extracted dye from the petals of the Flame of forest (*Butea monosperma*) flower. It was used for the extraction of phenolic substances by Gan and Latiff (2011) and Gong et al. (2012).

Kumar et al. (2014) used a rotatable central experimental design for drying processes, and optimised the hot air drying conditions of the okra with the help of a microwave oven. Han et al. (2010) optimised the process parameters of microwave vacuum drying for apple slices.

Some applications of the Central composite design in membrane technology and the food industry are summarised in Table 5.

## 4. CONCLUSIONS

In general, ultrafiltration examinations are performed with one variable method at a time, where the effect of each factor is examined separately. However, this approach results in a large number of experiments and can often ignore interaction effects. Furthermore, process optimisation is inefficient, as it is difficult to find the true optimum in a reasonable amount of experiments. The use of statistical methods such as the response surface methodology overcomes the limitations of the univariate simultaneous approach. RSM is an effective statistical tool that is also used in the field of membrane technology to model and optimise many process variables.

## ACKNOWLEDGEMENT

This study was financed by the Hungarian National Research, Development and Innovation Office, project NKFI-FK-142414. S. Kertész is grateful for the financial support of the János Bolyai Research Scholarship of the Hungarian Academy of Sciences (BO/00576/20/4).

## REFERENCES

Abhari, P., Abdi, S., and Nasiri, M. (2022). Effect of various types of anions and anionic surfactants on the performance of micellar-enhanced ultrafiltration process in the removal of  $Pb(II)$  ions: an optimization with the response surface methodology. *Chemical Engineering Research and Design*, 187: 332–346. <https://doi.org/10.1016/j.cherd.2022.09.020>.



Akal, C., Eminoğlu, G., and Özer, B. (2023). Optimisation of stabiliser usage conditions in oat milk production using response surface methodology. *Acta Alimentaria*, 52(1): 143–154. <https://doi.org/10.1556/066.2022.00263>.

Aloulou, H., Attia, A., Aloulou, W., Chakraborty, S., Baklouti, L., Dammak, L., and Amar, R. B. (2022). Statistical simulation, a tool for the process optimization of oily wastewater by crossflow ultrafiltration. *Membranes*, 12(7): 676. <https://doi.org/10.3390/membranes12070676>.

Alventosa-DeLara, E., Barredo-Damas, S., Alcaína-Miranda, M.I., and Iborra-Clar, M.I. (2014). Study and optimization of the ultrasound-enhanced cleaning of an ultrafiltration ceramic membrane through a combined experimental-statistical approach. *Ultrasonics Sonochemistry*, 21(3): 1222–1234. <https://doi.org/10.1016/j.ultsonch.2013.10.022>.

Anderson-Cook, C.M., Borror, C.M., and Montgomery, D.C. (2009). Response surface design evaluation and comparison. *Journal of Statistical Planning and Inference*, 139(2): 629–641. <https://doi.org/10.1016/j.jspi.2008.04.004>.

Ba, D. and Boyaci, I.H. (2007). Modeling and optimization i: usability of response surface methodology. *Journal of Food Engineering*, 78(3): 836–845. <https://doi.org/10.1016/j.jfoodeng.2005.11.024>.

Baklouti, S., Kamoun, A., Ellouze-Ghorbel, R., and Chaabouni, S. (2013). Optimising operating conditions in ultrafiltration fouling of pomegranate juice by response surface methodology. *International Journal of Food Science and Technology*, 48(7): 1519–1525. <https://doi.org/10.1111/ijfs.12120>.

Beg, S. (Ed.) (2021). *Design of experiments for pharmaceutical product development*. Springer Singapore. VII, p. 96. <https://link.springer.com/book/10.1007/978-981-33-4717-5>.

Bezerra, M.A., Santelli, R.E., Oliveira, E.P., Villar, L.S., and Escaleira, L.A. (2008). Response surface methodology (RSM) as a tool for optimization in analytical chemistry. *Talanta*, 76(5): 965–977, Elsevier. <https://doi.org/10.1016/j.talanta.2008.05.019>.

Box, G.E.P. and Behnken, D.W. (1960). Some new three level designs for the study of quantitative variables. *Technometrics*, 2(4): 455–475. <https://doi.org/10.1080/00401706.1960.10489912>.

Box, G.E.P. and Wilson, K.B. (1951). On experimental attainment of optimum conditions. *Journal of the Royal Statistical Society Series B (Methodological)*, 8: 1–38.

Candéa, T.V., Monteiro, F.S., Tonon, R.V., and Cabral, L.M.C. (2015). Effect of process variables on the production of flaxseed oil emulsions by cross-flow membrane emulsification. *Food Engineering Reviews*, 7(2): 258–264. <https://doi.org/10.1007/s12393-014-9085-8>.

Cojocaru, C. and Zakrzewska-Trznadel, G. (2007). Response surface modeling and optimization of copper removal from aqua solutions using polymer assisted ultrafiltration. *Journal of Membrane Science*, 298(1–2): 56–70. <https://doi.org/10.1016/j.memsci.2007.04.001>.

Dereli, R.K., van der Zee, F.P., Ozturk, I., and van Lier, J.B. (2019). Treatment of cheese whey by a cross-flow anaerobic membrane bioreactor: biological and filtration performance. *Environmental Research*, 168: 109–117. <https://doi.org/10.1016/j.envres.2018.09.021>.

Draper, N.R. and Lin, D.K.J. (1990). Small response-surface designs. *Technometrics*, 32(2): 187–194. <https://doi.org/10.2307/1268862>.

Fan, G., Han, Y., Gu, Z., and Chen, D. (2008). Optimizing conditions for anthocyanins extraction from purple sweet potato using response surface methodology (RSM). *LWT – Food Science and Technology*, 41(1): 155–160. <https://doi.org/10.1016/j.lwt.2007.01.019>.

Ferreira, S.L.C., Bruns, R.E., da Silva, E.G.P., dos Santos, W.N.L., Quintella, C.M., David, J.M., de Andrade, J.B., Breitkreitz, M.C., Jardim, I.C.S.F., and Neto, B.B. (2007). Statistical designs and response surface techniques for the optimization of chromatographic systems. *Journal of Chromatography A*, 1158(1–2): 2–14. <https://doi.org/10.1016/j.chroma.2007.03.051>.



Figueroa, R.A.R., Cassano, A., and Drioli, E. (2011). Ultrafiltration of orange press liquor: optimization for permeate flux and fouling index by response surface methodology. *Separation and Purification Technology*, 80(1): 1–10. <https://doi.org/10.1016/j.seppur.2011.03.030>.

Gan, C.Y. and Latiff, A.A. (2011). Optimisation of the solvent extraction of bioactive compounds from *Parkia speciosa* pod using response surface methodology. *Food Chemistry*, 124(3): 1277–1283. <https://doi.org/10.1016/j.foodchem.2010.07.074>.

Gong, Y., Hou, Z., Gao, Y., Xue, Y., Liu, X., and Liu, G. (2012). Optimization of extraction parameters of bioactive components from defatted marigold (*Tagetes erecta* L.) residue using response surface methodology. *Food and Bioproducts Processing*, 90(1): 9–16. <https://doi.org/10.1016/j.fbp.2010.12.004>.

Han, Q.H., Yin, L.J., Li, S.J., Yang, B.N., and Ma, J.W. (2010). Optimization of process parameters for microwave vacuum drying of apple lices using response surface method. *Drying Technology*, 28(4): 523–532. <https://doi.org/10.1080/07373931003618790>.

Hanrahan, G., Zhu, J., Gibani, S., and Patil, D.G. (2005). Chemometrics and statistics: experimental design. In: Worsfold, P.J., Townshend, A., and Poole, C.F. (Eds.), *Encyclopedia of analytical science*. Elsevier, C, pp. 8–12.

Kemény, S., Deák, A., Lakn  Komka, K., and Kunovszki, P. (2017). *K s rletek tervez se  s  rt kel se. (Design and evaluation of experiments)*. Typotex, pp. 322–355.

Krishnan, S., Suzana, B.N., Wahid, Z.A., Nasrullah, M., Abdul Munaim, M.S., Din, M.F.B.M., Taib, S.M., and Li, Y.Y. (2020). Optimization of operating parameters for xylose reductase separation through ultrafiltration membrane using response surface methodology. *Biotechnology Reports*, 27: e00498. <https://doi.org/10.1016/j.btre.2020.e00498>.

Kumar, D., Prasad, S., and Murthy, G.S. (2014). Optimization of microwave-assisted hot air drying conditions of okra using response surface methodology. *Journal of Food Science and Technology*, 51(2): 221–232. <https://doi.org/10.1007/s13197-011-0487-9>.

Kyll nen, H.M., Pirkonen, P., and Nystr m, M. (2005). Membrane filtration enhanced by ultrasound: a review. *Desalination*, 181(1–3): 319–335. <https://doi.org/10.1016/j.desal.2005.06.003>.

Landaburu-Aguirre, J., Pongr cz, E., Per m ki, P., and Keiski, R.L. (2010). Micellar-enhanced ultrafiltration for the removal of cadmium and zinc: use of response surface methodology to improve understanding of process performance and optimisation. *Journal of Hazardous Materials*, 180(1–3): 524–534. <https://doi.org/10.1016/j.jhazmat.2010.04.066>.

Leardi, R. (2009). Experimental design in chemistry: a tutorial. *Analytica Chimica Acta*, 652(1–2): 161–172. <https://doi.org/10.1016/j.aca.2009.06.015>.

Lin, W., Jing, L., and Zhang, B. (2020). Micellar-enhanced ultrafiltration to remove nickel ions: a response surface method and artificial neural network optimization. *Water (Switzerland)*, 12(5). <https://doi.org/10.3390/W12051269>.

Madaeni, S.S. and Samieirad, S. (2010). Chemical cleaning of reverse osmosis membrane fouled by wastewater. *Desalination*, 257(1–3): 80–86. <https://doi.org/10.1016/j.desal.2010.03.002>.

Malaisamy, R., Annadurai, G., and Mohan, D. (2000). Performance optimization of polysulfone ultrafiltration membranes for riboflavin separation using design experiments. *Bioprocess Engineering*, 22: 227–232. <https://doi.org/10.1007/s004490050724>.

Malekzadeh, H. and Fatemi, M.H. (2015). Analysis of flavor volatiles of some Iranian rice cultivars by optimised static headspace gas chromatography-mass spectrometry. *Journal of the Iranian Chemical Society*, 12(12): 2245–2251. <https://doi.org/10.1007/s13738-015-0703-z>.



Miao, J., Zhang, L.C., and Lin, H. (2013). A novel kind of thin film composite nanofiltration membrane with sulfated chitosan as the active layer material. *Chemical Engineering Science*, 87: 152–159. <https://doi.org/10.1016/j.ces.2012.10.015>.

Myers, R.H. and Montgomery, D.C. (1995). Response surface methodology: process and product optimization using designed experiments. In: *Wiley Series in probability and statistics applied probability and statistics*. Wiley, New York, pp. 856.

Nair, A.T., Makwana, A.R., and Ahammed, M.M. (2014). The use of response surface methodology for modelling and analysis of water and wastewater treatment processes: a review. *Water Science and Technology*, 69(3): 464–478. <https://doi.org/10.2166/wst.2013.733>.

Nekkanti, V., Muniyappan, T., Karatgi, P., Hari, M.S., Marella, S., and Pillai, R. (2009). Spray-drying process optimization for manufacture of drugcyclodextrin complex powder using design of experiments. *Drug Development and Industrial Pharmacy*, 35(10): 1219–1229. <https://doi.org/10.1080/03639040902882264>.

Otto, M. (1999). *Chemometrics: statistics and computer applications in analytical chemistry*. Wiley-VCH., p. 330.

Park, K.B., Choi, C., Yu, H.W., Chae, S.R., and Kim, I.S. (2018). Optimization of chemical cleaning for reverse osmosis membranes with organic fouling using statistical design tools. *Environmental Engineering Research*, 23(4): 474–484. <https://doi.org/10.4491/eer.2017.098>.

Peeva, P.D., Knoche, T., Pieper, T., and Ulbricht, M. (2012). Cross-flow ultrafiltration of protein solutions through unmodified and surface functionalized polyethersulfone membranes - effect of process conditions on separation performance. *Separation and Purification Technology*, 92: 83–92. <https://doi.org/10.1016/j.seppur.2012.03.013>.

Prakash Maran, J. and Manikandan, S. (2012). Response surface modeling and optimization of process parameters for aqueous extraction of pigments from prickly pear (*Opuntia ficus-indica*) fruit. *Dyes and Pigments*, 95(3): 465–472. <https://doi.org/10.1016/j.dyepig.2012.06.007>.

Sadeghian, M., Sadeghi, M., Hesampour, M., and Moheb, A. (2015). Application of response surface methodology (RSM) to optimize operating conditions during ultrafiltration of oil-in-water emulsion. *Desalination and Water Treatment*, 55(3): 615–623. <https://doi.org/10.1080/19443994.2014.919607>.

Salehi, R., Mousavi, S.M., and Taherian, M. (2019). Assessment of micellar-enhanced ultrafiltration process performance for removal of pharmaceutical contaminant from wastewater using response surface methodology. *International Journal of Environmental Science and Technology*, 16(10): 6199–6206. <https://doi.org/10.1007/s13762-018-2021-3>.

Shakir, N.A.A., Wong, K.Y., Noordin, M.Y., and Sudin, I. (2015). Development of a high performance PES ultrafiltration hollow fiber membrane for oily wastewater treatment using response surface methodology. *Sustainability (Switzerland)*, 7(12): 16465–16482. <https://doi.org/10.3390/su71215826>.

Sharma, A. and Bracewell, D.G. (2019). Characterisation of porous anodic alumina membranes for ultrafiltration of protein nanoparticles as a size mimic of virus particles. *Journal of Membrane Science*, 580: 77–91. <https://doi.org/10.1016/j.memsci.2019.02.071>.

Singh, B. and Beg, S. (2013). Quality by design in product development life cycle. *Cronicle Pharmabiz*, 22: 72–79.

Sinha, K., Saha, P.D., and Datta, S. (2012). Extraction of natural dye from petals of Flame of forest (*Butea monosperma*) flower: process optimization using response surface methodology (RSM). *Dyes and Pigments*, 94(2): 212–216. <https://doi.org/10.1016/j.dyepig.2012.01.008>.



Sivakumar, M., Annadurai, G., and Mohan, D. (1999). Studies on Box–Behnken design experiments: cellulose acetate-polyurethane ultrafiltration membranes for BSA separation. *Bioprocess Engineering*, 21: 65–68. <https://doi.org/10.1007/s004490050642>.

Tarley, C.R.T., Silveira, G., dos Santos, W.N.L., Matos, G.D., da Silva, E.G.P., Bezerra, M.A., Miró, M., and Ferreira, S.L.C. (2009). Chemometric tools in electroanalytical chemistry: methods for optimization based on factorial design and response surface methodology. *Microchemical Journal*, 92(1): 58–67. <https://doi.org/10.1016/j.microc.2009.02.002>.

Vani, M.M., Shruthi Keerthi, D., and Sridhar, S. (2023). Optimisation studies on removal of fluoride by micellar enhanced ultrafiltration. *Materials Today: Proceedings*, 72: 486–493. <https://doi.org/10.1016/j.matpr.2022.09.454>.

Wang, C., Wei, A., Wu, H., Qu, F., Chen, W., Liang, H., and Li, G. (2016). Application of response surface methodology to the chemical cleaning process of ultrafiltration membrane. *Chinese Journal of Chemical Engineering*, 24(5): 651–657. <https://doi.org/10.1016/j.cjche.2016.01.002>.

Wang, L., Yang, B., Du, X., Yang, Y., and Liu, J. (2008). Optimization of conditions for extraction of acid-soluble collagen from grass carp (*Ctenopharyngodon idella*) by response surface methodology. *Innovative Food Science and Emerging Technologies*, 9(4): 604–607. <https://doi.org/10.1016/j.ifset.2008.03.001>.

Xiarchos, I., Jaworska, A., and Zakrzewska-Trznadel, G. (2008). Response surface methodology for the modelling of copper removal from aqueous solutions using micellar-enhanced ultrafiltration. *Journal of Membrane Science*, 321(2): 222–231. <https://doi.org/10.1016/j.memsci.2008.04.065>.

Xie, J.H., Shen, M.Y., Xie, M.Y., Nie, S.P., Chen, Y., Li, C., Huang, D.F., and Wang, Y.X. (2012). Ultrasonic-assisted extraction, antimicrobial and antioxidant activities of *Cyclocarya paliurus* (Batal.) Iljin'skaja polysaccharides. *Carbohydrate Polymers*, 89(1): 177–184. <https://doi.org/10.1016/j.carbpol.2012.02.068>.

Xue, H.Y., Li, J.R., Liu, Y.G., Gao, Q., Wang, X.W., Zhang, J.W., Tanokura, M., and Xue, Y.L. (2019). Optimization of the ultrafiltration-assisted extraction of Chinese yam polysaccharide using response surface methodology and its biological activity. *International Journal of Biological Macromolecules*, 121: 1186–1193. <https://doi.org/10.1016/j.ijbiomac.2018.10.126>.

Yolmeh, M., Habibi Najafi, M.B., and Farhoosh, R. (2014). Optimisation of ultrasound-assisted extraction of natural pigment from annatto seeds by response surface methodology (RSM). *Food Chemistry*, 155: 319–324. <https://doi.org/10.1016/j.foodchem.2014.01.059>.

Zolgharnein, J., Shahmoradi, A., and Ghasemi, J.B. (2013). Comparative study of Box–Behnken, central composite, and Doehlert matrix for multivariate optimization of Pb (II) adsorption onto *Robinia* tree leaves. *Journal of Chemometrics*, 27(1–2): 12–20. <https://doi.org/10.1002/cem.2487>.

**Open Access statement.** This is an open-access article distributed under the terms of the Creative Commons Attribution 4.0 International License (<https://creativecommons.org/licenses/by/4.0/>), which permits unrestricted use, distribution, and reproduction in any medium, provided the original author and source are credited, a link to the CC License is provided, and changes – if any – are indicated. (SID\_1)

